Influence of a dual monsoon system and two sources of groundwater recharge on Kofu basin alluvial fans, Japan

Takashi Nakamura, Kei Nishida and Futaba Kazama

ABSTRACT

This study investigates the contribution ratios of different groundwater recharge sources and influence of a dual monsoon system in Kofu basin, central Japan, through the hydrogen and oxygen isotopic analysis of precipitation, river water, and groundwater. The study is focused on the area of the Kamanashigawa and Midaigawa alluvial fans, which are formed by two main rivers. Precipitation isotopic content exhibits significant seasonal variability. Also, river water presents *d*-excess values higher than annual precipitation at plain areas (9 and 10‰), suggesting that two different air-masses contribute to precipitation, corresponding to the monsoon and pre-monsoon periods. The results of this study allow estimation of relative contributions of different sources to groundwater and influence of a dual monsoon system. The mass-balance analysis of the $\delta^{18}O$ to identify the groundwater source indicates the river water contributes 38–100% of the recharge, while precipitation contributes 29–62% in Kamanashigawa alluvial fan. In the case of Midaigawa alluvial fan, river water contributes 77–99% in the northern part; in the southern side, 30–93% of contribution comes from precipitation. The mass-balance analysis of the *d*-excess indicates pre-monsoon precipitation contributes 46–68% and 39–65% to groundwater of the Kamanashigawa and Midaigawa alluvial fans, respectively.

Key words | alluvial fan, *d*-excess values, groundwater, hydrogen and oxygen isotopes of water, monsoon system

Takashi Nakamura (corresponding author)
Kei Nishida
Futaba Kazama
Interdisciplinary Center for River Basin Environment,
University of Yamanashi,
4-3-11 Takeda,
Kofu Yamanashi 400-8510,
Japan
E-mail: *tnakamura@yamanashi.ac.jp*

INTRODUCTION

Environmental tracers such as oxygen and hydrogen stable isotopes ($\delta^{18}O$ and δD) are commonly used in hydrological investigations, e.g., to estimate the groundwater recharge, to identify multiple recharge sources, and to investigate the interactions between the surface and groundwater, such as the flow paths and mixing in regional aquifers, advection/diffusion in groundwater aquifers, and the effects of evaporation on groundwater systems (Deshpande *et al.* 2003; Palmer *et al.* 2007). The values of $\delta^{18}O$ and δD remain constant as long as phase changes or fractionation does not occur along the flow path (Senturk *et al.* 1970; Perry *et al.* 1980; Clark & Fritz 1997). However, stable isotope fractionation occurs when the water changes its state (e.g., through evaporation or condensation, raindrop formation, and infiltration in aquifers). Consequently, the isotopic composition varies between the different forms of water (i.e., precipitation, surface water, and groundwater). A comparative analysis of the $\delta^{18}O$ and δD composition and spatiotemporal distribution of precipitation, river water, and groundwater provides a useful tool for evaluating recharge mechanism and defining the status of mixed groundwater recharge zones (Chen *et al.* 2006; Mukherjee *et al.* 2007; Negrel *et al.* 2011; Yeh *et al.* 2011; Liu & Yamanaka 2012; Peng *et al.* 2012).

To investigate groundwater recharge through stable isotope analysis, the measured $\delta^{18}O$ is plotted against δD, producing the 'local meteoric water line' (LMWL), which is then compared with the 'global meteoric water line'

doi: 10.2166/nh.2016.208

(GMWL, Craig 1961; Gat 1996). The deviations and their characteristics (e.g., slope and intercept) of the LMWL from the GMWL may be used to infer the groundwater recharge mechanism. The LMWL may vary due to evaporation and condensation (e.g., temperature and humidity), terrain environment, altitude, and other reasons. The intercept is also called deuterium excess or *d*-excess ($d = \delta D - 8.0\ \delta^{18}O$) (Dansgaard 1964). A globally representative *d*-excess is 10‰ (Craig 1961); however, it may vary depending on the evaporation conditions in the origin of the water source. For example, *d*-excess is 6.03 in North America and 3.97 in the Tropical Island area (Gat 1996). In Japan, *d*-excess in different seasons is reported to vary from 14.8 in April–September to 23.8 in October–March, even though the LMWL slope remains approximately the same (Liu & Yamanaka 2012). Comparing the differences in the stable isotopic signatures of groundwater, river water, and local precipitation allows the effect of different sources of groundwater recharge to be identified (Scanlon *et al.* 2002; Kalbus *et al.* 2006), whereas comparing the *d*-excess values of groundwater and precipitation between the different seasons allows identification of the effect of the dual monsoon (Yeh *et al.* 2011).

Rainwater characteristics in Japan are controlled by monsoon (summer, May–October) and pre-monsoon precipitation (winter, November–April). These two seasonal circulation systems are a part of the larger monsoon circulation in South Asia, and they are caused by seasonal temperature and pressure gradient reversal, which is associated with the wind circulation following the annual northward and southward motion of the sun. Normal precipitation *d*-excess values for the pre-monsoon and monsoon periods are greater than 20‰ and less than 10‰, respectively (Nakayama *et al.* 2000). Such seasonal variation is caused by the contribution of the dual moisture sources predominantly from the Pacific Ocean in summer with SE monsoon winds and predominantly from the Sea of Japan with NE monsoon winds in winter (Waseda & Nakai 1983; Araguás-Araguás *et al.* 1998). Yeh *et al.* (2011) estimated seasonal contributions of precipitation to groundwater recharge in the Chih-pen Creek basin of eastern Taiwan. However, very few studies that have examined the aspects have investigated both the recharge contribution from different sources and its temporal variability.

Groundwater is an important source of water for industrial, agricultural, and drinking water use in Kamanashgawa and Midaigawa alluvial fans, located in Kofu basin, because this rural area has no dams for surface water use. This basin is located in inland Japan and the distances from the Pacific Ocean and Sea of Japan are about 70 km and 160 km, respectively. The rainwater characteristics in this area are controlled by precipitation during the summer (SE) and winter (NE) monsoons. The SE monsoon operates during the months of May–October and NE pre-monsoon during the months of November–April. Therefore, in a local area such as the Kofu basin, the *d*-excess for the different seasons is expected to differ from the general values of Japan.

In this context, the study aims to identify the local oxygen and hydrogen stable isotopic characteristics and the relative contribution of the two groundwater sources (precipitation infiltration and river water recharge) and the dual monsoon system (pre-monsoon and monsoon seasons) on groundwater recharge in Kamanashi and Midai alluvial fans of the Kofu basin in the central part of Japan.

MATERIALS AND METHODS

The study area

Kofu Basin, located in central Japan, is drained by the Fuji River and surrounded by steep mountains of ~2,000 m (Figure 1). The Fuji River originates as the Kamanashi River from the north of the southern Alps and as the Fuefuki River from the north of the Kofu Basin. The Fuji River basin (area = 3,570 km^2) has a very complex and fragile geological substratum due to several dislocations in the area. Consequently, many parts of the basin have collapsed; the clastic sediments are transported by the river and accumulate in gentle flow areas. Due to the increased gravel and sand deposition, areas with elevations less than 500 m comprise compound alluvial fans formed by the Kamanashi and Fuefuki River tributaries (MLIT 2001). The average Kamanashi and Fuefuki River streamflows in the central Kofu basin are approximately 10 and 20 m^3/s, respectively, whereas that of Fuji River at the basin's outlet is approximately 72 m^3/s (Shrestha & Kazama 2007).

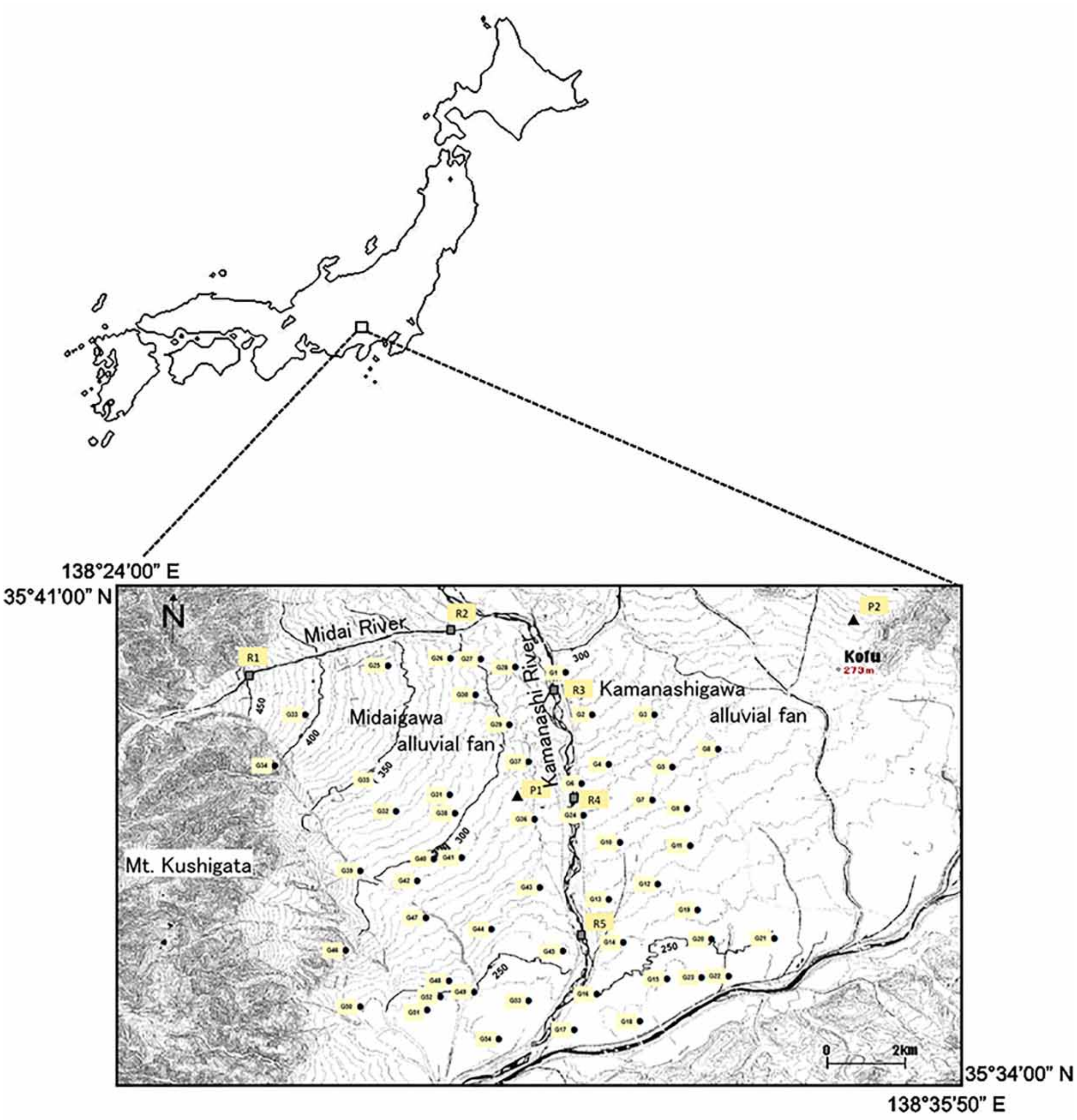

Figure 1 | Sampling sites of precipitation (squares), groundwater (black dots), and river water (gray dots).

The Midaigawa and Kamanashigawa alluvial fans (area $= 90\ \text{km}^2$) were formed in the western Kofu basin (Figure 1) due to sand and gravel deposition by the Midai and Kamanashi River, transported from steep mountain areas. The central and upper parts of the Kamanashigawa alluvial fan consist of gravel, with a depth of 75–95 m; the lower part is composed of clay soil, covered with gravel, with a depth of 15–25 m. The Midaigawa alluvial fan is formed of gravel, transported by the Midai River, without any clay soil. The Midai and Kamanashi riverbeds are raised above the Midaigawa and Kamanashigawa alluvial fans, due to sediment deposition inside the riverbanks (MLIT 2001).

Kofu basin lies in an inland region; therefore, its temperature exhibits extreme variations between summer and winter. The observed metrological data of the Japan Metrological Agency (JMA) (2008) indicates that typically, summers are hot and humid, and winters are cold, with average temperatures of 26 °C and 3 °C, respectively. Annual rainfall in Kofu basin is as little as 1,135 mm in the lower areas, but reaches up to 2,500 mm in the high stands. The entire basin receives a mean annual precipitation of approximately 2,100 mm; approximately 75% of the annual precipitation occurs during the monsoon season from May to October.

Sampling and chemical analysis

Monthly precipitation samples were collected in the period August 2003–July 2004 at a station (elevation = 250 m) in the Midaigawa alluvial fan (Figure 1, P1). Additionally, to determine the LMWL in this area, event-wise precipitation samples were acquired in the period March 2007–February 2008 at a station (elevation = 308 m) in University of Yamanashi premises, located approximately 6 km east of the Kamanashigawa alluvial fan (Figure 1, P2). All the precipitation samples were collected in polyethylene plastic bottles attached to funnels with an anti-evaporation cap. River water and groundwater samples were collected between January and December 2007 for chemical and isotopic (oxygen and hydrogen) analyses. Sampling was carried out during both wet and dry periods on a bimonthly basis from the rivers (Midai and Kamanashi) and from domestic wells (depth being 20–50 m) (Figure 1).

Hydrogen and oxygen isotope ratios were expressed as δD and δ^{18}O, respectively, where $\delta = [(R_{sample}/R_{standard}) - 1] \times 1000$ (‰), and R is D/H or ^{18}O/^{16}O in the sampled water (R_{sample}) or standard mean ocean water ($R_{standard}$). The δ^{18}O and δD were analyzed using an isotope ratio mass spectrometer (IRMS) (Sercon, ANCA20-20, UK) after establishing equilibrium with CO_2 gas for ^{18}O and H_2 gas for D. Each sample gas was extracted using an auto-sampling system (Sercon, WES, UK). The analytical precision was 0.1‰ for δ^{18}O and 1‰ for δD.

RESULTS

Precipitation isotopic compositions

The δ^{18}O and δD values of precipitation can provide important information about hydrogeological processes and atmospheric circulation. Table 1 presents the results of the stable isotope analyses in the two alluvial fans of Kofu basin, Japan. At P1, the δ^{18}O and δD significantly varies during August 2003–July 2004; the δ^{18}O values range from −14.1 to −6.8‰, and the δD values range from −90 to −42‰. The δ^{18}O and δD in the P2 samples acquired during March 2007–February 2008 also vary; δ^{18}O values range from −18.0 to −0.6‰, and δD values range from −134 to −1‰. However, the variability magnitude differs between the two sites (Table 1). Seasonal changes in δD and δ^{18}O are not expressed in these locations (Figure 2).

On the contrary, *d*-excess shows distinct seasonal variability. It generally ranges from 10 to 23‰. Relatively higher *d*-excess values (from 15 to 23‰) are detected corresponding to the pre-monsoon seasons (October–April 2003/2004), whereas they are low (10 to 11‰) for the monsoon seasons (August–September 2003 and May–July 2004) at location P1 (Figure 2(a)). The *d*-excess value of event-wise precipitation samples also suggests seasonal variability; pre-monsoon seasons (March 2007–April 2007 and October 2007–February 2008) are associated with a high frequency of increased *d*-excess values (>10‰), whereas the monsoon season (May–September 2007) exhibits a high-frequency of low *d*-excess values (<10‰) at location P2 (Figure 2(b)). These results are consistent with data reported by other researchers (e.g., Asano *et al.* 2002; Lee & Kim 2007; Yeh *et al.* 2011), which indicated that precipitation *d*-excess in Central Japan, Korea, and Eastern Taiwan has a distinct seasonal variability, high (>15‰) in the dry season and low in the wet season (<10‰).

To illustrate the isotopic data for the different seasons, two LMWLs are plotted using precipitation samples for a 12-month period, collected during August 2003–July 2004, and an additional 55 event-wise samples, collected during March 2007–February 2008 (Figure 3). The LMWLs for the pre-monsoon (October–April) and the monsoon (May–September) seasons are defined by the equations $\delta D = 8.0\ \delta^{18}O + 14.4$ and $\delta D = 8.0\ \delta^{18}O + 6.8$, respectively. The slope of both LMWLs is 8.0, which is identical to that of the GMWL reported by Craig (1961). The LMWLs' intercept (6.8 for monsoon LMWL and 14.4 for pre-monsoon LMWL) is identical to that of the MWL intercept (7 for monsoon and 16 for pre-monsoon) for the Nara basin in main island of Japan reported by Nakayama *et al.* (2000), as shown in Figure 3. The δ^{18}O (and δD) annual weighted

Table 1 | Stable isotopic composition and metrological data

Location	Collected day	Rain fall mm	Temperature °C	δD ‰	$\delta^{18}O$ ‰	*d*-excess ‰
P1	Aug-03	291	25.8	−55	−8.3	11
	Sep-03	164	23.7	−85	−12.0	11
	Oct-03	72	15.4	−42	−7.2	16
	Nov-03	157	13	−49	−8.6	20
	Dec-03	21	6.2	−42	−8.2	23
	Jan-04	13	2.8	−90	−14.1	22
	Feb-04	27	5.9	−50	−8.3	13
	Mar-04	55	8.1	−77	−11.4	15
	Apr-04	73	15.4	−76	−11.5	16
	May-04	113	20	−73	−10.5	11
	Jun-04	111	23.4	−66	−9.5	10
	Jul-04	49	27.9	−45	−6.8	10
P2	12-Mar-07	9	6.9	−43.7	−8.3	22
	26-Mar-07	10	12.7	−55.1	−8.1	10
	30-Mar-07	9	14.2	−26.4	−4.4	9
	09-Apr-07	4	12.3	−5.6	−2.7	16
	14-Apr-07	10	15.6	−27.4	−5.5	17
	19-Apr-07	21	9.7	−85.5	−11.9	10
	26-Apr-07	18	13.7	−55.0	−8.2	13
	30-Apr-07	6	11.6	−23.6	−4.3	11
	07-May-07	30	17.1	−74.2	−10.2	8
	11-May-07	4	17.5	−0.5	−0.6	4
	18-May-07	12	14.5	−103.9	−13.6	5
	26-May-07	25	16.5	−57.6	−8.4	9
	01-Jun-07	10	17.5	−40.0	−6.1	9
	09-Jun-07	13	19.3	−38.9	−6.1	10
	13-Jun-07	16	23.3	−54.8	−8.6	14
	15-Jun-07	7	19.3	−55.5	−7.3	3
	25-Jun-07	24	22.6	−71.3	−9.9	8
	01-Jul-07	13	24.9	−68.9	−9.0	3
	02-Jul-07	2	22.6	−60.8	−8.3	6
	05-Jul-07	12	23.8	−77.5	−10.5	6
	12-Jul-07	4	22.4	−44.1	−6.1	5
	13-Jul-07	11	22.7	−88.3	−11.3	2
	15-Jul-07	199	23.2	−117.0	−15.5	7
	18-Jul-07	48	22.7	−82.6	−11.4	8
	21-Jul-07	3	23.4	−38.7	−5.5	6
	23-Jul-07	48	26.8	−33.1	−5.4	10
	31-Jul-07	79	24.7	−75.5	−10.5	8
	17-Aug-07	35	29.4	−46.5	−6.8	8

(*continued*)

Table 1 | continued

Location	Collected day	Rain fall mm	Temperature °C	δD ‰	$\delta^{18}O$ ‰	*d*-excess ‰
	20-Aug-07	44	27.3	−53.5	−7.5	6
	26-Aug-07	45	26.7	−79.0	−10.5	5
	01-Sep-07	5	24.2	−51.5	−6.9	4
	07-Sep-07	195	25.9	−45.1	−6.2	5
	12-Sep-07	107	24.0	−75.4	−10.5	8
	25-Sep-07	21	23.6	−22.2	−4.0	10
	01-Oct-07	59	17.3	−41.1	−7.1	15
	05-Oct-07	11	17.8	−24.7	−4.7	13
	16-Oct-07	1	17.2	−12.9	−3.6	16
	21-Oct-07	30	14.8	−22.3	−5.5	22
	30-Oct-07	111	14.7	−124.5	−16.4	7
	31-Oct-07	7	16.7	−15.3	−3.2	10
	07-Nov-07	10	14.8	−49.5	−7.5	11
	12-Nov-07	10	13.7	−35.4	−6.2	14
	04-Dec-07	2	5.6	−28.9	−5.4	15
	12-Dec-07	1	6.5	−33.7	−5.3	9
	14-Dec-07	12	8.9	−38.2	−6.9	17
	23-Dec-07	27	6.2	−109.6	−15.8	16
	31-Dec-07	40	5.8	−74.2	−11.1	15
	14-Jan-08	7	2.5	−31.2	−4.8	7
	22-Jan-08	2	0.3	−115.5	−15.2	6
	24-Jan-08	12	2.0	−68.6	−10.2	13
	04-Feb-08	24	2.5	−134.2	−18.0	10
	06-Feb-08	1	0.5	−74.3	−11.2	18
	11-Feb-08	16	2.5	−72.0	−12.7	29
	13-Feb-08	6	2.0	−62.1	−10.1	18
	27-Feb-08	8	2.5	−77.3	−11.6	15

mean values of the precipitation samples from P1 and P2 are −9.5‰ (−66‰) and −10.1 (−72‰), respectively.

River water isotopic compositions

The bimonthly river water $\delta^{18}O$ and δD from both alluvial fans does not present significant temporal variations relative to the values measured in the precipitation samples. The $\delta^{18}O$ (δD) is essentially constant in the Midai River at a value of −11.3 ± 0.12‰ (−77 ± 1.1‰) upstream (Table 2, R1) and at −10.9 ± 0.14‰ (−75 ± 1.6‰) downstream (Table 2, R2). In the case of the Kamanashi River, the values are −11.0 ± 0.13‰ (−76 ± 0.9‰) upstream (Table 2, R3), −10.9 ± 0.07‰ (−76 ± 0.7‰) middlestream (Table 2, R4), and −11.0 ± 0.14‰ (−76 ± 0.7‰) downstream (Table 2, R5). Spatial variations of $\delta^{18}O$ and δD are insignificant for both rivers, probably due to lack of inflow. Additionally, $\delta^{18}O$ and δD are less than the mean values in the precipitation samples ($\delta^{18}O$ = −9.5‰ and −10.1‰, δD = −62.5‰ and −7.2‰). The fact that the alluvial fans are located in a range of altitudes (200 to 500 m), lower than those of the average catchment, suggests that altitude may affect $\delta^{18}O$ and δD values. The river water *d*-excess value (11–13‰, Table 2) is higher than the annual precipitation *d*-excess values (9 and 10‰).

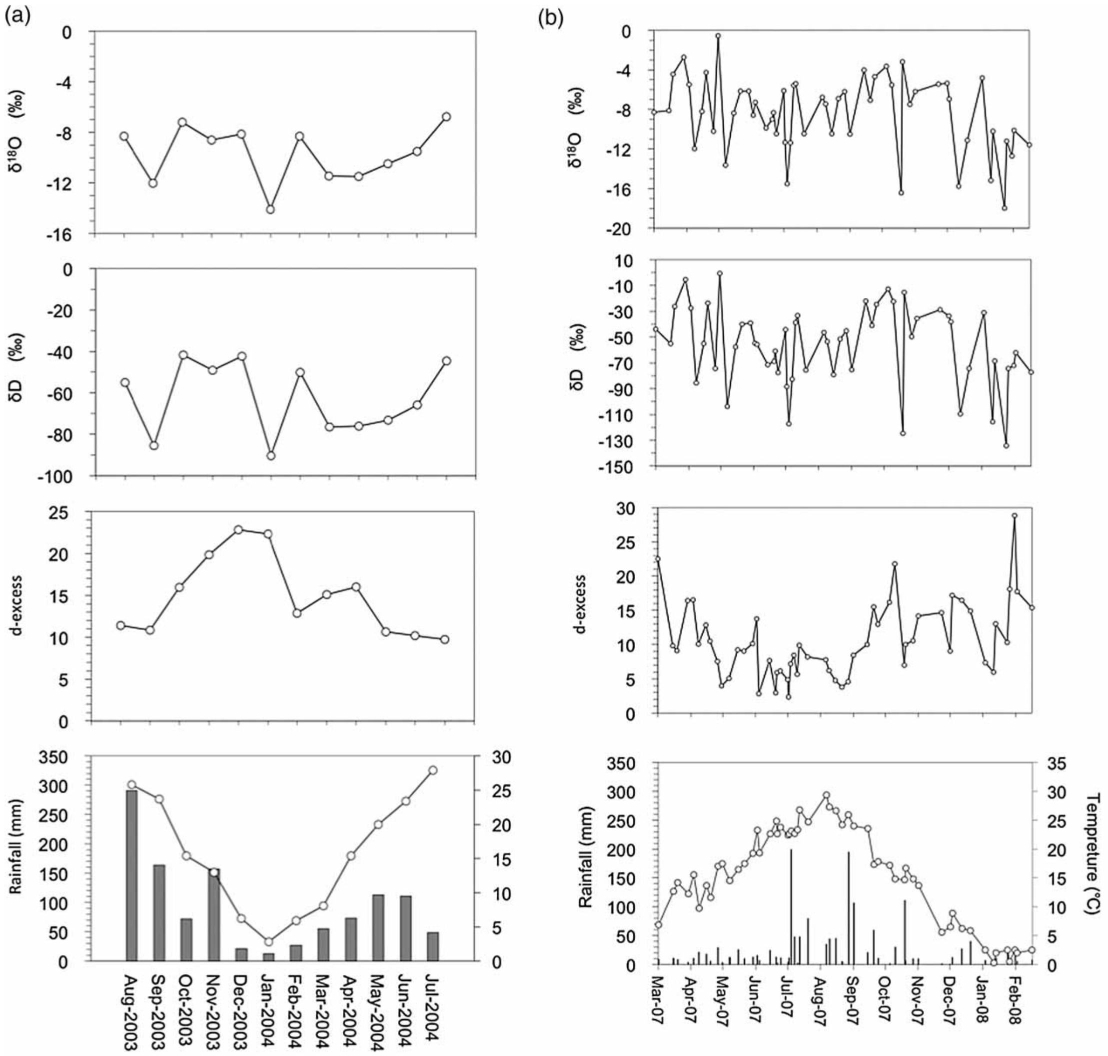

Figure 2 | Temporal variations of δD, $\delta^{18}O$, *d*-excess, rainfall amount, and temperature of precipitation at the lower part of Kofu basin: P1 (a) and P2 (b).

Isotopic compositions of groundwater

The δD and $\delta^{18}O$ values in the groundwater samples do not exhibit any seasonal variation; the standard deviations for the two seasons are below 1.5‰ and 0.2‰, respectively (Table 2). However, relatively wide spatial variation is found in the groundwater annual mean isotope values, with $\delta^{18}O$ ranging from −11.0 to −9.9‰ and δD from −76 to −69‰ in the Midai alluvial fan. For the Kamanashigawa alluvial fan, $\delta^{18}O$ and δD were in the range of −11.1 to −10.3‰ and −77 to −71‰, respectively (Table 2). In terms of spatial distribution, the $\delta^{18}O$ is relatively low toward the Kamanashi River side of both alluvial fans, whereas higher values are detected towards the central and the eastern part of the Midaigawa and the Kamanashigawa alluvial fan, respectively (Figure 4).

The annual mean δD and $\delta^{18}O$ plots for groundwater, river water, and precipitation are presented in Figure 5, along with the LMWLs for the monsoon and the pre-monsoon seasons. The groundwater isotopic values from both alluvial fans apparently deviate from the LMWLs in both seasons. The regression line's slope is 6.5, different from that of the LMWL.

The distribution of *d*-excess in groundwater and river water is shown in Figure 6. Relatively high groundwater *d*-excess values are detected toward the Kamanashi River

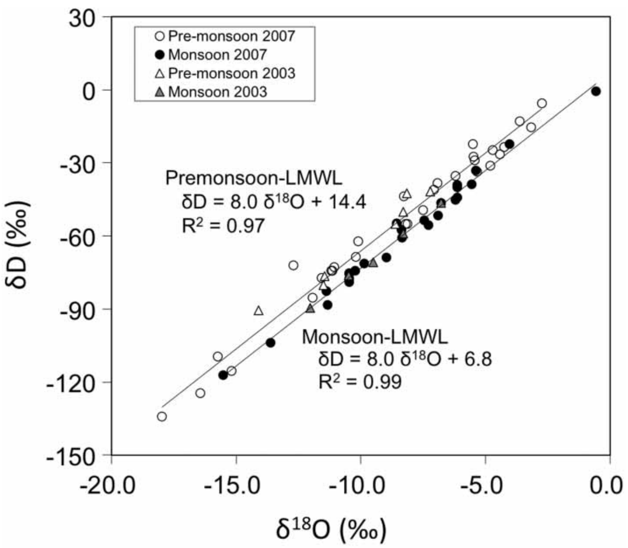

Figure 3 | Plot of δD against $\delta^{18}O$ for the precipitation samples.

side of the alluvial fans. On the other hand, relatively lower *d*-excess values are measured in the central area of the Midaigawa and in the eastern part of the Kamanashigawa alluvial fan. Previous researchers have reported a positive correlation between rainwater *d*-excess values and altitude (Rindsberger *et al.* 1990; Cruz San Julian *et al.* 1992).

DISCUSSION

Precipitation and river water isotopic differences

The results of the present study illustrate that precipitation values $\delta^{18}O$ and δD exhibit a wide temporal variability (Figure 2), unlike river water and groundwater $\delta^{18}O$ and δD values (Table 2). The isotopic fractionation by the rainfall recharge significantly affects the groundwater isotopic values. However, the amplitude of the seasonal fraction for the isotopic values in groundwater is expected to decrease with increasing residence time (Maloszewski & Zuber 1993; Asano *et al.* 2002). Asano *et al.* (2002) reported the relationship between the estimated residence time of the spring water and amplitude of the isotopic fractionation. It shows, in the case of groundwater with more than 1 year residence time, the isotopic amplification pattern will not have a significant regression. In addition, Mizutani *et al.* (2001) hypothesized that if the groundwater system is predominantly recharged through infiltration of precipitation, the groundwater isotopic composition will directly reflect the isotopic values of precipitation.

The two-river water (Midai and Kamanashi River) is represented by depleted isotopic composition rather than the weighted average of isotopic composition of precipitation at plain areas. The maximum altitudes of the Midai and Kamanashi River watersheds are approximately 2,400 m and 2,500 m, respectively. Therefore, it is possible that the different isotopic values between river water and precipitation result from this altitude difference. This hypothesis is further corroborated by previously reported evidence such as the depletion in surface water annual mean $\delta^{18}O$ and δD values compared with the precipitation weighted mean in alluvial fans; and the decreasing of surface water ^{18}O and D content with increasing altitude (Dansgaard 1964; Siegenthaler & Oeschger 1980; Poage & Chamberlain 2001; Yeh *et al.* 2011; Liu & Yamanaka 2012). Waseda & Nakai (1983) also indicated the altitude effect as an important factor determining the surface and meteoric waters' isotopic compositions in central and northeast Japan, and they reported an average altitude effect on surface water $\delta^{18}O$ and δD values in those areas as −0.25‰ and −2.0‰ per 100 m, respectively.

In the plain area, river water *d*-excess exhibits a higher value (11–13‰) than the annual precipitation (9 and 10‰), suggesting the evaporation effects on different elevations or two air-masses contributed to the precipitation event, one with a monsoon precipitation (low *d*-excess) and one with a pre-monsoon precipitation (high *d*-excess).

Seasonal variation of *d*-excess values of precipitation samples

The *d*-excess is defined as the excess deuterium that cannot be accounted by equilibrium fractionation between water and vapor. Since condensation is most often an equilibrium process, *d*-excess is an indicator of kinetic fractionation during evaporation, governed by molecular diffusivity of isotopic molecular species (Dansgaard 1964; Clark & Fritz 1997). Although temperature and wind speed can influence the kinetic fractionation, relative humidity is the most important factor. The *d*-excess of the GMWL has a value of ~10 representing evaporation at ~85% relative humidity.

Table 2 | Annual mean values and standard deviation of δD, $\delta^{18}O$, and *d*-excess for bimonthly groundwater and river water samples

Sample	ID	Fan/Location	Latitude	Longitude	$\delta^{18}O$, Ave ± SD ‰	δD, Ave ± SD ‰	*d*-excess, Ave ± SD ‰
G.W.	G1	Kamanashigawa	35°39′47.42″	138°30′17.35″	−10.9 ± 0.08	−76 ± 0.5	12 ± 0.5
	G2	Kamanashigawa	35°39′11.83″	138°30′39.76″	−11.1 ± 0.09	−77 ± 0.7	12 ± 0.6
	G3	Kamanashigawa	35°39′11.82″	138°31′32.6″	−10.6 ± 0.15	−74 ± 1.2	11 ± 0.4
	G4	Kamanashigawa	35°38′.97″	138°30′54″	−10.8 ± 0.11	−76 ± 0.5	11 ± 0.7
	G5	Kamanashigawa	35°38′.92″	138°31′.52″	−10.6 ± 0.13	−74 ± 1.1	11 ± 0.4
	G6	Kamanashigawa	35°38′13.78″	138°30′31.25″	−11.0 ± 0.16	−76 ± 1.4	12 ± 0.7
	G7	Kamanashigawa	35°37′59.91″	138°31′.52″	−10.7 ± 0.06	−74 ± 0.4	11 ± 0.3
	G8	Kamanashigawa	35°38′.84″	138°32′.99″	−10.3 ± 0.13	−71 ± 0.9	11 ± 0.4
	G9	Kamanashigawa	35°37′52.86″	138°31′59.97″	−10.4 ± 0.12	−73 ± 0.8	10 ± 0.3
	G10	Kamanashigawa	35°37′24.02″	138°31′.21″	−10.6 ± 0.04	−74 ± 0.6	11 ± 0.5
	G11	Kamanashigawa	35°37′21.18″	138°32′.48″	−10.6 ± 0.08	−74 ± 0.6	11 ± 0.3
	G12	Kamanashigawa	35°36′49.09″	138°31′.48″	−10.9 ± 0.10	−76 ± 0.4	12 ± 0.6
	G13	Kamanashigawa	35°36′36.09″	138°30′.91″	−10.9 ± 0.10	−76 ± 0.9	11 ± 0.3
	G14	Kamanashigawa	35°35′59.68″	138°31′.07″	−10.7 ± 0.08	−75 ± 1.0	11 ± 0.5
	G15	Kamanashigawa	35°35′.81″	138°31′.86″	−10.9 ± 0.07	−76 ± 0.5	11 ± 0.5
	G16	Kamanashigawa	35°35′16.07″	138°30′.64″	−10.8 ± 0.06	−76 ± 0.8	11 ± 0.5
	G17	Kamanashigawa	35°34′.84″	138°30′.65″	−10.8 ± 0.14	−75 ± 1.1	12 ± 0.5
	G18	Kamanashigawa	35°34′.08″	138°31′.27″	−10.9 ± 0.10	−76 ± 0.6	11 ± 0.4
	G19	Kamanashigawa	35°36′.13″	138°32′.74″	−11.1 ± 0.10	−77 ± 0.6	12 ± 0.9
	G20	Kamanashigawa	35°36′.66″	138°32′.5″	−11.0 ± 0.12	−76 ± 0.3	12 ± 0.7
	G21	Kamanashigawa	35°36′.98″	138°33′.42″	−10.9 ± 0.08	−76 ± 0.6	12 ± 0.6
	G22	Kamanashigawa	35°35′.51″	138°32′.82″	−10.9 ± 0.12	−76 ± 0.9	11 ± 0.5
	G23	Kamanashigawa	35°35′.21″	138°32′.25″	−10.9 ± 0.06	−75 ± 0.4	12 ± 0.3
	G24	Kamanashigawa	35°37′.02″	138°30′.64″	−11.0 ± 0.14	−76 ± 1.1	11 ± 0.6
	G25	Midaigawa	35°39′.53″	138°27′.73″	−10.9 ± 0.07	−75 ± 0.8	12 ± 0.3
	G26	Midaigawa	35°39′.64″	138°28′.65″	−11.0 ± 0.10	−76 ± 0.9	12 ± 0.7
	G27	Midaigawa	35°39′.94″	138°29′.86″	−10.8 ± 0.12	−76 ± 1.0	11 ± 1.2
	G28	Midaigawa	35°39′.93″	138°29′.3″	−10.8 ± 0.12	−75 ± 0.7	11 ± 1.0
	G29	Midaigawa	35°39′.71″	138°29′.21″	−10.8 ± 0.16	−75 ± 1.2	11 ± 0.9
	G30	Midaigawa	35°39′28.54″	138°29′1.82″	−10.7 ± 0.14	−75 ± 1.0	11 ± 0.9
	G31	Midaigawa	35°38′4.21″	138°28′40″	−10.4 ± 0.20	−73 ± 1.4	10 ± 0.8
	G32	Midaigawa	35°37′.4″	138°27′.69″	−10.2 ± 0.16	−71 ± 1.5	10 ± 0.9
	G33	Midaigawa	35°39′.86″	138°26′.31″	−10.9 ± 0.06	−76 ± 0.4	12 ± 0.5
	G34	Midaigawa	35°38′.97″	138°26′.5″	−9.9 ± 0.10	−69 ± 0.9	10 ± 0.6
	G35	Midaigawa	35°38′.93″	138°27′38.3″	−10.6 ± 0.11	−73 ± 0.9	11 ± 1.3
	G36	Midaigawa	35°37′.86″	138°29′.4″	−10.6 ± 0.06	−74 ± 0.6	11 ± 0.5
	G37	Midaigawa	35°38′.18″	138°29′46.31″	−10.8 ± 0.02	−75 ± 0.8	12 ± 0.9
	G38	Midaigawa	35°37′.67″	138°28′.33″	−10.2 ± 0.16	−71 ± 0.8	11 ± 0.6
	G39	Midaigawa	35°37′.35″	138°27′.58″	−10.1 ± 0.11	−70 ± 0.8	10 ± 0.9
	G40	Midaigawa	35°37′.08″	138°28′.57″	−10.1 ± 0.14	−71 ± 0.8	10 ± 0.8

(*continued*)

Table 2 | continued

Sample	ID	Fan/Location	Latitude	Longitude	$\delta^{18}O$, Ave ± SD ‰	δD, Ave ± SD ‰	*d*-excess, Ave ± SD ‰
	G41	Midaigawa	35 °37′.38″	138 °28′.04″	−10.3 ± 0.10	−72 ± 0.4	10 ± 1.0
	G42	Midaigawa	35 °36′.93″	138 °28′.53″	−10.4 ± 0.14	−72 ± 1.1	11 ± 0.7
	G43	Midaigawa	35 °36′.95″	138 °29′.05″	−10.5 ± 0.10	−73 ± 0.7	12 ± 1.4
	G44	Midaigawa	35 °36′.76″	138 °29′.02″	−10.2 ± 0.05	−71 ± 0.7	11 ± 0.9
	G45	Midaigawa	35 °35′.22″	138 °30′.14″	−10.6 ± 0.13	−75 ± 0.5	11 ± 0.8
	G46	Midaigawa	35 °35′.98″	138 °27′.12″	−10.0 ± 0.16	−69 ± 0.5	10 ± 0.8
	G47	Midaigawa	35 °36′.56″	138 °28′.5″	−10.2 ± 0.09	−71 ± 1.2	11 ± 1.0
	G48	Midaigawa	35 °35′.21″	138 °28′.12″	−10.1 ± 0.15	−71 ± 1.5	10 ± 0.9
	G49	Midaigawa	35 °35′.09″	138 °29′.33″	−10.3 ± 0.12	−73 ± 1.2	10 ± 0.7
	G50	Midaigawa	35 °35′.61″	138 °27′24.22″	−10.2 ± 0.21	−71 ± 1.1	10 ± 0.8
	G51	Midaigawa	35 °35′.71″	138 °28′.94″	−10.6 ± 0.10	−74 ± 0.9	10 ± 0.9
	G52	Midaigawa	35 °35′.72″	138 °28′.74″	−10.5 ± 0.17	−74 ± 0.9	10 ± 1.2
	G53	Midaigawa	35 °35′.76″	138 °29′.49″	−10.4 ± 0.14	−72 ± 1.1	11 ± 1.1
	G54	Midaigawa	35 °34′.16″	138 °29′.33″	−10.4 ± 0.11	−72 ± 0.9	11 ± 0.9
River water	R1	Midaigawa Riv.	35 °39′29.65″	138 °25′34.65″	−11.3 ± 0.12	−77 ± 1.1	13 ± 1.1
	R2	Midaigawa Riv.	35 °40′.53″	138 °28′43.03″	−10.9 ± 0.14	−75 ± 1.6	12 ± 0.8
	R3	Kamanashigawa Riv.	35 °39′.62″	138 °30′6.92″	−11.0 ± 0.13	−76 ± 0.9	12 ± 1.1
	R4	Kamanashigawa Riv.	35 °38′.05″	138 °30′19.13″	−10.9 ± 0.07	−76 ± 0.7	11 ± 0.3
	R5	Kamanashigawa Riv.	35 °35′38.95″	138 °30′33.01″	−11.0 ± 0.14	−76 ± 0.7	11 ± 1.0

Figure 4 | Spatial distribution of $\delta^{18}O$ values in groundwater samples.

However, the *d*-excess value in the regional precipitation can be greater than ten if the evaporation in the source region takes place under lower humidity (Gat & Carmi 1970).

The *d*-excess in precipitation was generally higher in winter (d > 10) and lower in summer in Japan. Dansgaard (1964) and Waseda & Nakai (1983) have stated that the extremely high *d*-excess that appeared in Japanese precipitation

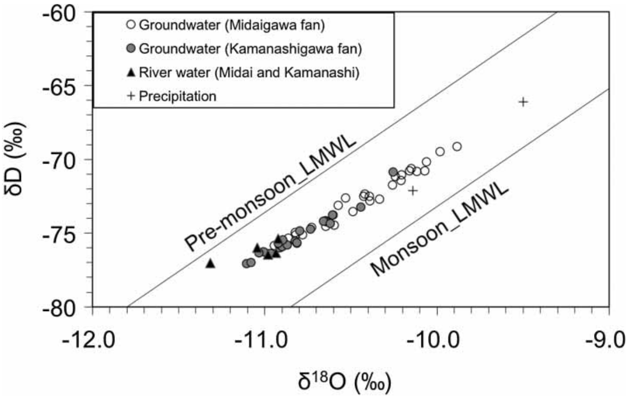

Figure 5 | Plots of δD against $\delta^{18}O$ of the groundwater, river water, and weighted mean values for the precipitation samples.

during the winter season resulted from rapid evaporation induced by dry, continental air masses brought from the Sea of Japan. In the case of the meteoric condition, the winter season dominates NE pre-monsoon winds. The resultant precipitation will have high *d*-excess in Japan. Katsuyama *et al.* (2015) have studied a seasonal variation of *d*-excess values of precipitation at three locations crossing a main island of Japan; Sea of Japan side (Tottori prefecture), Sea of Japan side (Shiga prefecture), and Pacific Ocean side (Nara prefecture). The climate conditions are clearly different among these stations. In the Sea of Japan side (Tottori prefecture), much snow falls from December to March with low air temperatures. In Shiga, there is less snowfall but much more rainfall during summer. Summer rainfall is more plentiful in the Pacific Ocean side (Nara prefecture). However, similar sinusoidal *d*-excess variations in precipitation were repeated at these three stations, i.e., higher during winter and lower during summer. The sinusoidal pattern is caused by the contribution of the dual moisture sources predominantly from the Pacific Ocean in summer and predominantly from the Sea of Japan in winter (Waseda & Nakai 1983; Araguás-Araguás *et al.* 1998). Tase *et al.* (1997) also reported that this seasonal pattern was commonly observed at six stations in Kanto, Shikoku, and Kyushu regions in Japan. Hence, it can be inferred that dominant moisture sources are a significant influence on the seasonal variation of *d*-excess values in precipitation in our study area as well.

Identification of groundwater recharge sources and their mixing

Various recharge sources for alluvial aquifer systems are identified by groundwater and recharge isotopic and chemical characteristics (Vanderzalm *et al.* 2011). Plotting $\delta^{18}O$ versus δD (Figure 5) shows that groundwater samples from the Midaigawa and Kamanashigawa alluvial fans fall between river water and weighted average precipitation,

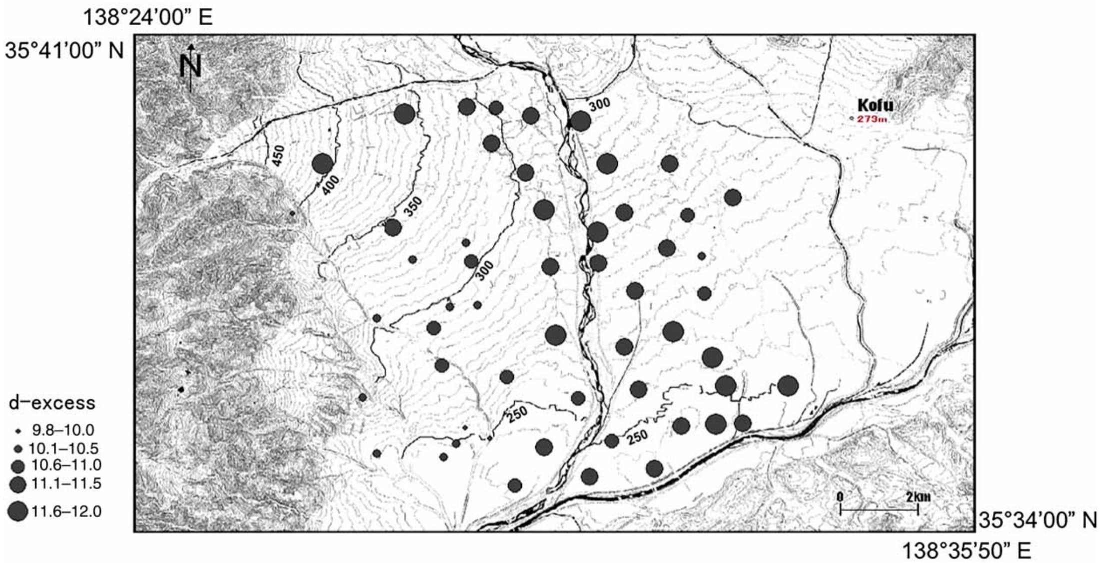

Figure 6 | Spatial distribution of the *d*-excess values in the groundwater samples.

indicating a possibility of recharge from both sources and their mixing in the aquifer.

The greater negativity of the $\delta^{18}O$ in the shallow groundwater samples toward the Midai River side in the Kamanashigawa alluvial fan (Figure 4) and the virtually identical $\delta^{18}O$ in the groundwater and river water toward the riverside of the Midai and Kamanashi Rivers in the Midaigawa alluvial fan, both suggest groundwater recharge from the rivers. On the other hand, samples most enriched in $\delta^{18}O$ and δD, having values of −9.9‰ and −69‰, respectively, are found in the groundwater (G34), well located at an altitude (490 m) higher than the riverbed perimeter (460 m). These values are close to the annual mean $\delta^{18}O$ and δD values of precipitation in the Midaigawa alluvial fan (−9.5‰ and −66‰), suggesting that precipitation is the primary source of groundwater at G34. Such high $\delta^{18}O$ values of groundwater were also detected in the eastern part of the Kamanashigawa alluvial fan and southern part of the Midaigawa alluvial fan. This isotopic distribution suggests that the groundwater in this area might be recharged through precipitation infiltration.

From the above discussions, it is clear that groundwater in the alluvial fans is recharged from both river water drained from mountain and direct precipitation infiltrates; however, each source's contribution may spatially vary within the study area. To reveal any mixing of the different sources of groundwater in the aquifer, *d*-excess values of annual precipitation, river water, and groundwater are plotted against $\delta^{18}O$ (Figure 7). The values of the groundwater samples plotted between those of precipitation and river water samples suggests that the *d*-excess varies according to mixing between river water and annual precipitation.

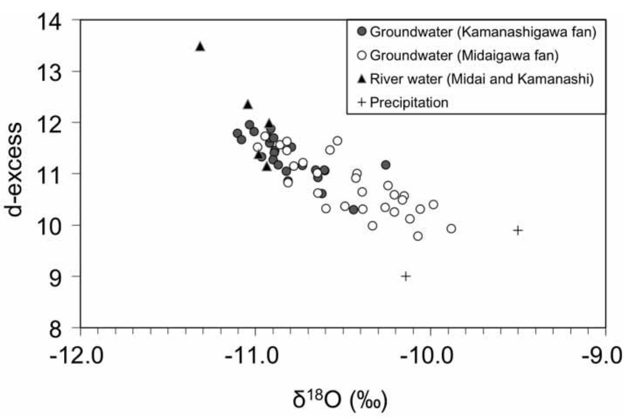

Figure 7 | Plot of *d*-excess and $\delta^{18}O$ values of the groundwater, river water, and precipitation samples.

Contribution of the different sources and timing of the groundwater recharge

The relative contributions to the groundwater recharge from the two distinct sources (i.e., precipitation and river water), which are important in water-budget studies, are inferred through the mass-balance analysis of the groundwater, river water, and precipitation isotopic values corresponding to different seasons from their *d*-excess values. To estimate the contribution of each source, this study considers a mass-balance of δ using a simple linear mixing model shown in Equations (1) and (2):

$$\delta_{groundwater} = X_{riverwater}\delta_{riverwater} + X_{precipitation}\delta_{precipitation}, \quad (1)$$

$$X_{riverwater} + X_{precipitation} = 1, \quad (2)$$

Equations (1) and (2) can convert to Equation (3) as below:

$$\delta_{groundwater} = X_{riverwater}\delta_{riverwater} + (1 - X_{riverwater})\delta_{precipitation}, \quad (3)$$

where $X_{river\ water}$ and $(1 - X_{river\ water})$ are the contribution of river water and precipitation infiltration, respectively. We used averaged $\delta^{18}O$ values of Kamanashigawa River and Midaigawa River water for $\delta_{river\ water}$ (Table 3). For the $\delta_{precipitation}$ we used averaged $\delta^{18}O$ values of precipitation samples at P1 and P2 (Table 3). Calculations based on Equations (1) and (2) in the wells considered in this study

Table 3 | Averaged values of isotope data of river water and precipitation samples

	X	Kamanashi alluvial fan	Midai alluvial fan
$X_{river\ water}$	$\delta^{18}O$ (‰)	−11.0	−11.1
$X_{precipitation}$	$\delta^{18}O$ (‰)	−9.8	−9.8
$X_{pre\text{-}monsoon}$	*d*-excess	14.4	14.4
$X_{monsoon}$	*d*-excess	6.8	6.8

Table 4 | Calculated values of contribution for river water and precipitation infiltration in groundwater samples and also pre-monsoon and monsoon contributions

ID	Fan/Location	Latitude	Longitude	$X_{river\ water}$ %	$X_{precipitation}$ %	$X_{pre\text{-}monsoon}$ %	$X_{monsoon}$ %
G1	Kamanashigawa	35°39′47.42″	138°30′17.35″	93	7	67	33
G2		35°39′.83″	138°30′39.76″	100	0	66	34
G3		35°39′.82″	138°31′.6″	67	33	56	44
G4		35°38′.97″	138°30′54″	85	15	56	44
G5		35°38′27.92″	138°31′47.52″	70	30	54	46
G6		35°38′.78″	138°30′.25″	100	0	66	34
G7		35°37′.91″	138°31′.52″	71	29	56	44
G8		35°38′.84″	138°32′.99″	38	62	58	42
G9		35°37′.86″	138°31′.97″	53	47	46	54
G10		35°37′24.02″	138°31′3.21″	67	33	56	44
G11		35°37′21.18″	138°32′.48″	68	32	50	50
G12		35°36′.09″	138°31′.48″	93	7	63	37
G13		35°36′.09″	138°30′.91″	91	9	61	39
G14		35°35′59.68″	138°31′.07″	78	22	57	43
G15		35°35′28.81″	138°31′.86″	91	9	61	39
G16		35°35′16.07″	138°30′.64″	85	15	53	47
G17		35°34′45.84″	138°30′24.65″	83	17	62	38
G18		35°34′.08″	138°31′.27″	92	8	59	41
G19		35°36′27.13″	138°32′.74″	100	0	64	36
G20		35°36′.66″	138°32′.5″	100	0	68	32
G21		35°36′.98″	138°33′.42″	93	7	64	36
G22		35°35′.51″	138°32′34.82″	89	11	57	43
G23		35°35′.21″	138°32′.25″	91	9	64	36
G24		35°37′.02″	138°30′.64″	97	3	60	40
G25	Midaigawa	35°39′53.53″	138°27′.73″	88	12	63	37
G26		35°39′59.64″	138°28′40.65″	99	1	62	38
G27		35°39′.94″	138°29′.86″	85	15	53	47
G28		35°39′.93″	138°29′35.3″	85	15	61	39
G29		35°39′3.71″	138°29′30.21″	82	18	57	43
G30		35°39′28.54″	138°29′.82″	77	23	58	42
G31		35°38′4.21″	138°28′40″	49	51	46	54
G32		35°37′.4"	138°27′54.69″	34	66	45	55
G33		35°39′.86″	138°26′38.31″	95	5	65	35
G34		35°38′28.97″	138°26′12.5″	7	93	41	59
G35		35°38′16.93″	138°27′38.3″	64	36	61	39
G36		35°37′43.86″	138°29′51.4″	70	30	55	45
G37		35°38′32.18″	138°29′46.31″	85	15	64	36
G38		35°37′48.67″	138°28′44.33″	37	63	52	48
G39		35°37′0.35″	138°27′24.58″	22	78	46	54

(*continued*)

Table 4 | continued

ID	Fan/Location	Latitude	Longitude	$x_{river\ water}$ %	$x_{precipitation}$ %	$x_{pre\text{-}monsoon}$ %	$x_{monsoon}$ %
G40		35°37′10.08″	138°28′26.57″	26	74	44	56
G41		35°37′.38″	138°28′50.04″	38	62	47	53
G42		35°36′.93″	138°28′12.53″	49	51	51	49
G43		35°36′.95″	138°29′56.05″	61	39	64	36
G44		35°36′10.76″	138°29′15.02″	29	71	50	50
G45		35°35′.22″	138°30′15.14″	70	30	50	50
G46		35°35′.98″	138°27′12.12″	15	85	47	53
G47		35°36′.56″	138°28′19.5″	34	66	50	50
G48		35°35′.21″	138°28′39.12″	23	77	39	61
G49		35°35′18.09″	138°29′0.33″	44	56	42	58
G50		35°35′.61″	138°27′24.22″	30	70	49	51
G51		35°35′.71″	138°28′20.94″	66	34	46	54
G52		35°35′13.72″	138°28′31.74″	57	43	47	53
G53		35°35′.76″	138°29′46.49″	52	48	55	45
G54		35°34′38.16″	138°29′21.33″	52	48	54	46

indicate that the contribution of river water from mountain watersheds to groundwater recharge ranges from 38% to 100% in the Kamanashigawa alluvial fan and from 7% to 99% in Midaigawa (Table 4). Although this suggests a relatively higher contribution of river water (originating from the mountain watershed) to the groundwater recharge in the Kamanashigawa alluvial fan, the wider range of contribution in different locations exemplifies their non-uniform distribution throughout the alluvial fans. Cluster analysis of the contributions from the two sources within the study area (Figure 8) demonstrates that in the central part of Kamanashigawa (locations G3, G5, G7, G8, G9, G10, and G11), precipitation contributes 29–62%; its contribution tends to increase with the distance from the

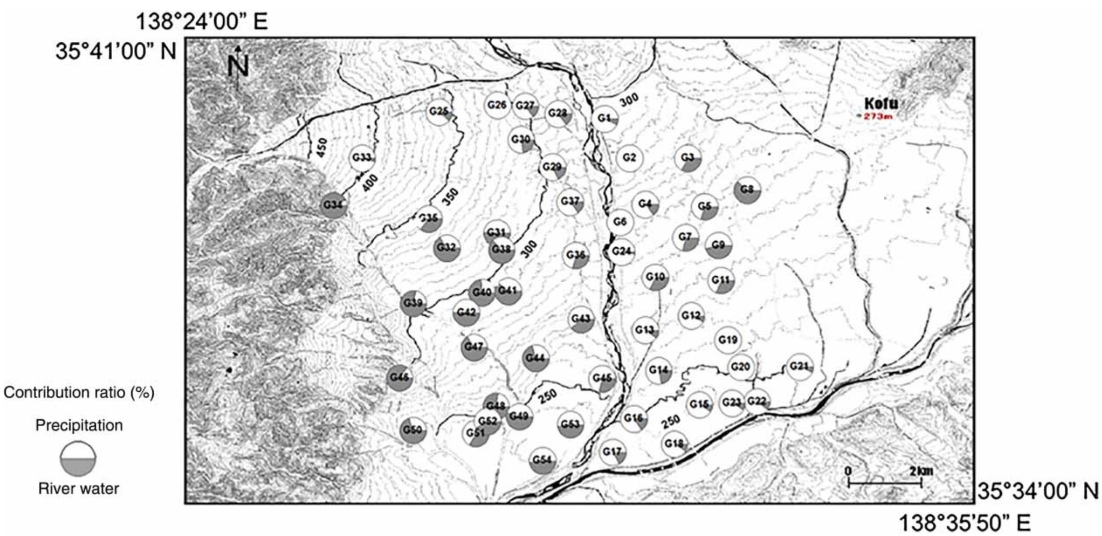

Figure 8 | Spatial distribution of groundwater recharge sources contribution ratios.

Kamanashi River. In the case of Midaigawa, river water and precipitation recharge differs greatly between the different regions. The northern region (within 2 km from the Midai and Kamanashi rivers, locations G25, G26, G27, G28, G29, G30, G33, and G37) receives 77–99% from river water, whereas the southern region (adjacent to Kushigata Mountain, G32, G38, G39, G40, G41, G42, G44, G46, G47, G48, and G50) receives 51–85% from precipitation.

To identify the seasonal variability between the contribution between the two sources (i.e., pre-monsoon and monsoon), a mass-balance of mean *d*-excess values using Equations (4) and (5) is considered:

$$d_{groundwater} = X_{pre-monsoon} d_{pre-monsoon} + X_{monsoon} d_{monsoon}, \quad (4)$$

$$X_{pre-monsoon} + X_{monsoon=} 1, \quad (5)$$

Equations (4) and (5) can convert to Equation (6) as below:

$$\delta_{groundwater} = X_{pre\text{-}monsoon} d_{pre\text{-}monsoon} + (1 - X_{pre\text{-}monsoon}) d_{monsoon}, \quad (6)$$

where $X_{pre\text{-}monsoon}$ and $(1 - X_{pre\text{-}monsoon})$ are the contribution of pre-monsoon and monsoon precipitations, respectively. The *d*-excess values are using the intercept of LMWL in pre-monsoon and monsoon for $d_{pre\text{-}monsoon}$ and $d_{pre\text{-}monsoon}$, respectively (Table 3). On the basis of this equation, the estimated contribution ratios of pre-monsoon and monsoon precipitations to the groundwater are presented in Figure 9. The precipitation during the pre-monsoon and monsoon seasons contributes 46–68% and 32–54%, respectively, in groundwater recharge of the Kamanashigawa alluvial fan. In the case of Midaigawa, the contributions in the pre-monsoon and monsoon seasons are 39–65% and 35–61%, respectively (Table 4).

CONCLUSIONS

The present study reveals the influence of the presence of two sources and seasonal variability on groundwater recharge in the alluvial fans of the Kofu basin, Japan. The alluvial fans are recharged from two sources: the river water drained by mountainous catchments and direct infiltration of precipitation in the plain area. The isotopic data indicate that river waters are isotopically lighter, whereas altitude effects become evident in the precipitation isotope values. In the Kamanashigawa alluvial fan, river water contributes 38–100% of the recharge, while precipitation contributes 29–62% in the central part and increases its

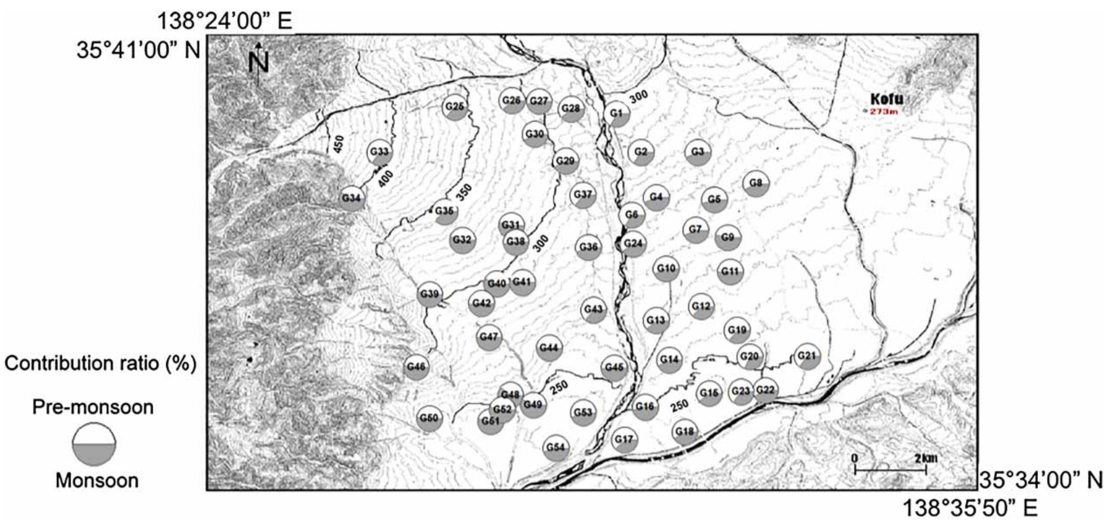

Figure 9 | Spatial distribution of the contribution ratios of the monsoon and pre-monsoon precipitation for groundwater.

contribution with distance from the Kamanashi River. In the case of Midaigawa, river water contributes 77–99% in the northern part, while in the southern side 30–93% of contribution comes from precipitation. Comparing the *d*-excess with $\delta^{18}O$ values reveals mixing of the river water with precipitation in the alluvial fan aquifer. Variation in precipitation and river water *d*-excess values, in the plains of the study area, suggests that pre-monsoon precipitation in the mountain areas (e.g., in the form of snow) might contribute more in recharge. The mass-balance analysis of the *d*-excess in groundwater and precipitation of different seasons (i.e., pre-monsoon and monsoon) indicates pre-monsoon precipitation contributes 46–68% and 39–65% to the groundwater recharge of Kamanashigawa and Midaigawa alluvial fans, respectively.

Notably, the pre-monsoon precipitation contribution to the groundwater recharge is more than 39%, while the total precipitation on the plain area in the same season is only 25% of the annual precipitation. This requirement could be met by pre-monsoon precipitation in the mountain area, which is carried by the river and recharged in the form of river water. Therefore, even if the annual precipitation amount in the plain area of the alluvial fans is quite small, the pre-monsoon precipitation could play an important role in recharging the groundwater, especially in the case of mountainous watersheds.

ACKNOWLEDGEMENTS

We are grateful to all members of the Water Quality Research Group of Interdisciplinary Center For River Basin Environment, University of Yamanashi. This study was supported by the Global Centres of Excellence (GCOE) program and Grant-in-Aids for Scientific Research (C) (No. 25630226) of the Japan Society for Promotion of Science (JSPS).

REFERENCES

Araguás-Araguás, L., Froehlich, K. & Rozanski, K. 1998 Stable isotope composition of precipitation over southeast Asia. *J. Geophys. Res.* **103**, 28721–28742.

Asano, Y., Uchida, T. & Ohte, N. 2002 Residence times and flow paths of water in steep unchannelled catchments, Tanakami, Japan. *J. Hydrol.* **261**, 173–192.

Chen, J., Tang, C. & Yu, J. 2006 Use of ^{18}O, ^{2}H and ^{15}N to identify nitrate contamination of groundwater in a wastewater irrigated field near the city of Shijiazhuang, China. *J. Hydrol.* **326**, 367–378.

Clark, I. D. & Fritz, P. 1997 *Environmental Isotopes in Hydrology*. Lewis, New York, USA.

Craig, H. 1961 Isotopic variations in meteoric waters. *Science* **133**, 1702–1703.

Cruz San Julian, J., Araguas, L., Rozanski, K., Benavente, J., Cardenal, J., Hidalgo, M. C., García López, S., Martinez Garrido, J. C., Moral, F. & Olias, M. 1992 Sources of precipitation over South-Eastern Spain and groundwater recharge. An isotopic study. *Tellus* **44**, 226–236.

Dansgaard, W. 1964 Stable isotopes in precipitation. *Tellus* **16**, 436–468.

Deshpande, R. D., Bhattacharya, R. A. & Gupta, S. K. 2003 Distribution of oxygen and hydrogen isotopes in shallow groundwaters from Southern India: influence of a dual monsoon system. *J. Hydrol.* **271**, 226–239.

Gat, J. R. 1996 Oxygen and hydrogen isotopes in the hydrologic cycle. *Annu. Rev. Earth Planet Sci.* **24**, 225–262.

Gat, J. R. & Carmi, I. 1970 Evolution of the isotopic composition of atmospheric waters in the Mediterranean Sea area. *J. Geophys. Res.* **75**, 3039–3048.

Japan Meteorological Agency. 2008 *Meteorological database*. Available at: http://www.data.jma.go.jp/obd/stats/etrn/index.php/ (accessed 1 August 2015).

Kalbus, E., Reinstorf, F. & Schirmer, M. 2006 Measuring methods for groundwater–surface water interactions: a review. *Hydrol. Earth Syst. Sci.* **10**, 873–887.

Katsuyama, M., Yoshioka, T. & Konohira, E. 2015 Spatial distribution of oxygen-18 and deuterium in stream waters across the Japanese archipelago. *Hydrol. Earth Syst. Sci.* **19**, 1577–1588.

Lee, K. S. & Kim, Y. 2007 Determining the seasonality of groundwater recharge using water isotopes: a case study from the upper North Han River basin, Korea. *Environ. Geol.* **52**, 853–859.

Liu, Y. & Yamanaka, T. 2012 Tracing groundwater recharge sources in a mountain–plain transitional area using stable isotopes and hydrochemistry. *J. Hydrol.* **464–465**, 116–126.

Maloszewski, P. & Zuber, A. 1993 Principles and practice of calibration and validation of mathematical models for the interpretation of environmental tracer data. *Adv. Water Resour.* **16**, 173–190.

Mizutani, Y., Satake, H., Yamabe, A., Miyachi, H., Mase, N. & Yamaura, K. 2001 Hydrogen and oxygen isotope ratios of groundwaters in shallow aquifer beneath the alluvial fan. *Journal of Groundwater Hydrology* **43** (1), 3–11 (in Japanese with English abstract).

MLIT 2001 *A Report of Boring Investigation in the Fuji Riverbed*. Ministry of Land, Infrastructure and Transport, Japan (in Japanese).

Mukherjee, A., Fryar, E. A. & Rowe, D. H. 2007 Regional-scale stable isotopic signatures of recharge and deep groundwater in the arsenic affected areas of West Bengal, India. *J. Hydrol.* **334**, 151–161.

Nakayama, T., Taniguchi, M. & Shimada, J. 2000 Characteristics of stable isotope ratios in precipitation and groundwater in Lake Biwa basin, Japan. *Japanese Journal of Limnology* **61**, 119–128 (in Japanese with English abstract).

Negrel, P. H., Pauwels, H., Dewandel, B., Gandolfi, J. M., Mascré, C. & Ahmed, S. 2011 Understanding groundwater systems and their functioning through the study of stable water isotopes in a hard-rock aquifer (Maheshwaram watershed, India). *J. Hydrol.* **397**, 55–70.

Palmer, C. P., Gannett, W. M. & Hinkle, R. S. 2007 Isotopic characterization of three groundwater recharge sources and inferences for selected aquifers in the upper Klamath Basin of Oregon and California, USA. *J. Hydrol.* **336**, 17–29.

Peng, T. R., Huang, C. C., Wang, C. H., Liu, T. K., Lu, W. C. & Chen, K. Y. 2012 Using oxygen, hydrogen, and tritium isotopes to assess pond water's contribution to groundwater and local precipitation in the pediment tableland areas of northwestern Taiwan. *J. Hydrol.* **450–451**, 105–106.

Perry, E. C., Grundl, T. & Gilkeson, R. H. 1980 H, O, S isotopic study of the groundwater in the Cambrian–Ordovician aquifer system of northern Illinois. In: *Isotope Studies of Hydrologic Processes* (E. C. Perry & C. W. Montgomery, eds). Northern Illinois University, Illinois, USA, pp. 35–43.

Poage, A. M. & Chamberlain, P. C. 2001 Empirical relationships between elevation and the stable isotope composition of precipitation and surface waters: consideration for studies of paleoelevation change. *Am. J. Sci.* **301**, 1–15.

Rindsberger, M., Jaffe, Sh., Rahamin, Sh. & Gat, J. R. 1990 Patterns of the isotopic composition of precipitation in time and space: data from the Israeli storm water collection program. *Tellus* **42**, 263–271.

Scanlon, R. B., Healy, W. R. & Cook, G. P. 2002 Choosing appropriate techniques for quantifying groundwater recharge. *Hydrogeol. J.* **10**, 18–39.

Senturk, F., Bursali, S., Omay, Y., Ertan, I., Guler, S., Yalcin, H. & Onhan, E. 1970 Isotope techniques applied to groundwater movement in the Konia plain. In: *Isotope Hydrology*, IAEA, Vienna, pp. 153–161.

Shrestha, S. & Kazama, F. 2007 Assessment of surface water quality using multivariate statistical techniques: a case study of the Fuji river basin, Japan. *Environ. Modell. & Softw.* **22**, 464–475.

Siegenthaler, U. & Oeschger, H. 1980 Correlation of ^{18}O in precipitation with temperature and altitude. *Nature* **285**, 189–223.

Tase, N., Shimano, Y., Kono, T., Mori, K., Shinmi, O., Yokoyama, S., Miyazawa, T., Kodama, Y., Matsumoto, E., Fushiwaki, Y., Ya-suike, S., Iijima, T., Kobayashi, M., Yamanaka, T. & Shimada, J. 1997 Isotopic variations in precipitation of Japan. In: *Proceedings of International Workshop on Global Change and Terrestrial Environment in Monsoon Asia*, Chiba University, Japan, pp. 140–143.

Vanderzalm, J. L., Jeuken, B. M., Wischusen, J. D. H., Pavelic, P., Le Gal La Salle, C., Knapton, A. & Dillon, P. J. 2011 Recharge sources and hydrogeochemical evolution of groundwater in alluvial basins in arid central Australia. *J. Hydrol.* **397**, 71–82.

Waseda, A. & Nakai, N. 1983 Isotopic composition of meteoric and surface waters in Central and Northeast Japan. *Geochemistry* **17**, 83–91 (in Japanese with English abstract).

Yeh, H. F., Lee, C. H. & Hsu, K. C. 2011 Oxygen and hydrogen isotopes for the characteristics of groundwater recharge: a case study from the Chin-Pen Creek basin, Taiwan. *Environ. Earth Sci.* **62**, 393–402.

First received 21 October 2015; accepted in revised form 6 June 2016. Available online 17 August 2016